

Theoretical Models of Highly Magnetic White Dwarf Stars with Non-Polytropic Equation of State

Hridaya Shah, Kunnat Sebastian

Department of Physics & Applied Physics, University of Massachusetts, Lowell, MA, USA

Email: hridaya_shah@uml.edu, kunnat_sebastian@uml.edu

How to cite this paper: Shah, H. and Sebastian, K. (2020) Theoretical Models of Highly Magnetic White Dwarf Stars with Non-Polytropic Equation of State. *Journal of Modern Physics*, 11, 1466-1491. <https://doi.org/10.4236/jmp.2020.119090>

Received: August 21, 2020

Accepted: September 27, 2020

Published: September 30, 2020

Copyright © 2020 by author(s) and Scientific Research Publishing Inc.

This work is licensed under the Creative Commons Attribution International License (CC BY 4.0).

<http://creativecommons.org/licenses/by/4.0/>



Open Access

Abstract

Super-massive white dwarf (WD) stars in the mass range 2.4 - 2.8 solar masses are believed to be the progenitors of “super-luminous” Type Ia supernovae according to a hypothesis proposed by some researchers. They theorize such a higher mass of the WD due to the presence of a very strong magnetic field inside it. We revisit their first work on magnetic WDs (MWDs) and present our theoretical results that are very different from theirs. The main reason for this difference is in the use of the equation of state (EoS) to make stellar models of MWDs. An electron gas in a magnetic field is Landau quantized and hence, the resulting EoS becomes non-polytropic. By constructing models of MWDs using such an EoS, we highlight that a strong magnetic field inside a WD would make the star super-massive. We have found that our stellar models do indeed fall in the mass range given above. Moreover, we are also able to address an observational finding that the mean mass of MWDs are almost double that of non-magnetic WDs. Magnetic field changes the momentum-space of the electrons which in turn changes their density of states (DOS), and that in turn changes the EoS of matter inside the star. By correlating the magnetic DOS with the non-polytropic EoS, we were also able to find a physical reason behind our theoretical result of super-massive WDs with strong magnetic fields. In order to construct these models, we have considered different equations of state with at most three Landau levels occupied and have plotted our results as mass-radius relations for a particular chosen value of maximum Fermi energy. Our results also show that a multiple Landau-level system of electrons leads to such an EoS that gives multiple branches in the mass-radius relations, and that the super-massive MWDs are obtained when the Landau-level occupancy is limited to just one level. Finally, our theoretical results can be explained solely on the basis of quantum and statistical mechanics that warrant no assumptions regarding stars.

Keywords

White Dwarf Star, Magnetic Field, Landau Levels, Equation of State, Density of States

1. Introduction

Recently, several observations of “peculiar” Type Ia supernovae: SN 2003fg, SN 2006gz, SN 2007if, SN 2009dc seem to indicate that their progenitor stars might be super-massive WDs with masses in the range 2.4 - 2.8 solar masses (M_{\odot}). This mass range clearly exceeds the Chandrasekhar mass limit of $1.44 M_{\odot}$ [1] [2] [3] [4]. These supernovae are different from the more common Type Ia supernovae in that they are more luminous and the ejected matter has lower kinetic energy than that observed in a regular supernova which suggests that the ancestor is most likely a WD star that is more massive than a WD of $1.44 M_{\odot}$ —a super-Chandrasekhar mass progenitor [5]. Some researchers have called for careful screening of Type Ia supernova events in future cosmology studies due to a possible SN sample contamination from such over-luminous supernovae events; while others suggest the need for a possible reconsideration of the expansion history of the Universe [5] [6].

In their very first work on the MWDs, Das & Mukhopadhyay have hypothesized the existence of very strong magnetic fields inside the WD in order to explain such a higher mass of the star [7]. Also, recently several WDs have been discovered that have surface magnetic fields in the range 10^5 to 10^9 G [8] [9] [10] [11] [12]. Nearly 10% of all WDs are found to be magnetic with fields in excess of $\sim 10^6$ G and that the mean mass of their mass distribution is $\sim 0.93 M_{\odot}$, while that of non-magnetic WDs is $\sim 0.56 M_{\odot}$ [12]. The presence of such high surface fields can lead us to hypothesize the existence of stronger interior fields, that although cannot be probed directly, to be quite a few orders of magnitude higher. This limit is set by the scalar virial theorem [13]

$$2T + W + 3\Pi + M = 0 \quad (1)$$

where T is the rotational energy, W the gravitational energy, Π the internal energy and M the magnetic energy. T and Π are both positive but W is negative, therefore the maximum magnetic energy M can be comparable to W but cannot be more than it in an equilibrium condition as is seen argued in Ref. [13].

For a star of mass M and radius R , this gives us $\frac{4\pi R^3}{3} \times \frac{B_{max}^2}{8\pi} \sim \frac{GM^2}{R}$ or

$B_{max} \sim 2 \times 10^8 (M/M_{\odot})(R/R_{\odot})^{-2}$ G for the average maximum interior B -field, and for the WDs this limit turns out to be $\sim 10^{12}$ G [13].

Successful magnetic WD models with $B \sim 10^{12}$ G at the center but with a vanishing field at the surface have been constructed by Ostriker & Hartwick [14]. Such a strong field can also be a consequence of a “frozen-in” field concept, also known as the flux conservation phenomenon, according to which the magnetic

flux of a star is more or less conserved throughout its evolution and its eventual collapse to becoming a degenerate star [15] [16]. Also, Ferrario & Wickramasinghe argue, on the assumption of flux conservation, that certain main-sequence stars such as A_p and B_p stars with fields in the range $\sim 200 - 25,000$ G can evolve into MWDs with dipolar fields in the range $\sim 10^6 - 10^9$ G, and this field range belongs to the vast majority of known MWDs [17].

Here, we consider a strongly magnetized, relativistic, completely degenerate electron gas at $T = 0$ K. The star is assumed to be spherically symmetric and the magnetic field is assumed to be static and uniform throughout the star. The purpose here is to study the effect of strong magnetic field on the momentum-space (p -space) and DOS of electrons as well as on the EoS of matter within the star, and then obtain the mass-radius relation of such a magnetized white dwarf star. Because the electrons within the star are considered to be relativistic (except possibly those in the density regions of a thin outer crust of a WD), we choose such values of B -field that are higher than a critical value which is given by equating the cyclotron energy of the electron to its rest mass energy [13],

$$\hbar\omega_c = mc^2 \quad (2)$$

where m is the mass and ω_c is the cyclotron frequency of the electron corresponding to the critical B -field and is given by

$$\omega_c = \frac{eB_{cr}}{mc}. \quad (3)$$

Therefore, the critical magnetic field is given by

$$B_{cr} = \frac{m^2 c^3}{\hbar e} = 4.414 \times 10^{13} \text{ G}. \quad (4)$$

Central field values of about $10^{12.3}$ G could be possible due to the aforementioned flux conservation if the progenitor of WD originally had a high magnetic field of the order 10^8 G to begin with [18]. The collapse of such a star into a degenerate remnant would dramatically increase the interior magnetic field since the total flux, $\phi \propto BR^2$, is more or less conserved. Central field " B_{cen} " in excess of 10^3 G has been theoretically proved to be possible within a MWD in the case of an electron gas occupying only one Landau level [19]. So, it does seem reasonable to hypothesize fields $\geq 10^{13}$ G. Although such high interior fields seem too extreme, there can be interesting consequences by assuming much stronger magnetic fields of the order of 10^{13-15} G, as is presented in this work.

In the presence of a magnetic field, an electron gas will be Landau quantized. Here, we study the effect of magnetic field on a system of relativistic, degenerate electrons that occupy at most three Landau levels. We also address the possibility of having super-massive WDs, having very strong, static and uniform magnetic field throughout, that violate the Chandrasekhar limit. We do this by making stellar models of MWDs from a "non-polytropic" EoS and find that our theoretical results do concur with the observations.

Normally, one makes such models of WDs from a polytropic relation, which relates pressures with density, of the form $P = K\rho^\Gamma$, where $\Gamma = \frac{n+1}{n}$. This is a simple power-law that works very well for a non-magnetic WD. In their work, Das & Mukhopadhyay (DM) have done piece-wise polytropic fits to the non-polytropic EoS of the MWD and have incorrectly assumed each individual fit, with particular values of K and Γ , to hold throughout the star. This is how DM have made models of MWDs [7]. We believe this to be an improper approach in dealing with a “non-polytropic” EoS. Not only that but a justification of their results of super-massive MWDs, from a fundamental perspective, is missing in their work. We have not done such piece-wise fits in our work and have also succeeded in providing an elementary explanation of our findings by correlating the electron momentum-space and the DOS with the EoS, and eventually, with the mass-radius relations of MWDs.

We have organized this paper as follows. In the next section, §2, we discuss the relevant equations and procedures necessary to construct models of MWDs and to correlate everything. In §3, we emphasize on the correlation between the plots of the EoS and those of the DOS. In §4, our numerical results are presented in the form of plots of mass-radius relations and a table summarizing all the mass-radius values. In the ensuing section, §5, we discuss the significant changes that take place in the momentum-space of electrons in presence of a magnetic field and correlate that to the DOS. More explanation for the super-Chandrasekhar WD star is given in §6. A comparison with the non-magnetic results is provided in §7, wherein we have retrieved the Chandrasekhar mass limit when $B \rightarrow 0$, *i.e.*, in the weak-field limit. In §8, we compare our results with those of Das & Mukhopadhyay and summarize the shortcomings in DM’s methods. Lastly, we conclude our results in §9.

2. Relevant Equations of a Cold, Degenerate Relativistic Free Electron Gas in a Magnetic Field

On solving the relativistic Dirac equation, one obtains the energy eigenvalues of a free electron in an external static and uniform magnetic field oriented in the z -direction, which are given by [13]

$$E_{\nu, p_z} = \left[p_z^2 c^2 + m^2 c^4 \left(1 + 2\nu \frac{B}{B_{cr}} \right) \right]^{\frac{1}{2}} \quad (5)$$

where

$$\nu = n + \frac{1}{2} + \frac{1}{2} \sigma_z \quad (6)$$

is the Landau quantum number and can take on values $\nu = 0, 1, 2, \dots$ which are known as Landau levels. Here, $n = 0, 1, 2, \dots$ is the principal quantum number and $\sigma_z = \pm 1$ is the spin quantum number or the spin of the electron. The electrons can become relativistic in either of the following two ways [13].

- 1) the cyclotron energy of the electron exceeds its rest mass energy
- 2) the density is so high that the mean Fermi energy of an electron exceeds its rest mass energy.

The first possibility gives us the definition of the critical magnetic field B_{cr} given in Equation (4). In the absence of a magnetic field, the density of states $g(E)$ per unit volume, denoted by $g^*(E)$ is given by,

$$g^*(E) = \frac{g(E)}{V} = \frac{dn_e}{dE} = \frac{8\pi}{h^3 c^3} E (E^2 - m^2 c^4)^{\frac{1}{2}} \tag{7}$$

which can be integrated from $E = mc^2$ to $E = E_F$, where E_F is the Fermi energy of the electrons, to get the number density of electrons n_e ,

$$n_e = \frac{8\pi}{3h^3 c^3} (E_F^2 - m^2 c^4)^{\frac{3}{2}} \tag{8}$$

Due to the presence of the magnetic field B , the DOS per unit volume becomes

$$g^*(E) = \frac{dn_e}{dE} = \frac{2b}{(2\pi)^2 \lambda^3} \sum_{\nu=0}^{\nu_m} D_{\nu} \frac{E}{mc^2 \sqrt{E^2 - m^2 c^4 (1 + 2\nu b)}} \Theta [E^2 - m^2 c^4 (1 + 2\nu b)] \tag{9}$$

where $b = \frac{B}{B_{cr}}$ is the dimensionless magnetic field, $\lambda = \frac{\hbar}{mc}$ is the Compton wavelength of an electron, Θ is the Heaviside function and D_{ν} is the degeneracy of the Landau level ν such that $D_{\nu} = 1$ for $\nu = 0$ and $D_{\nu} = 2$ for $\nu \geq 1$.

It just so happens that the above equation resembles the equation of the DOS of a quantum wire [20] with the exception that the Fermi gas in a quantum wire is, of course, non-relativistic. In a quantum wire, an electron gas is confined in two dimensions (say x and y -directions) but can move freely in the z -direction. Classically speaking, in a MWD, we essentially have the same situation of an electron confined in two dimensions (circular orbit) and free moving in the third dimension.

The upper limit of the summation can be found by setting $p_F^2 \geq 0$ in the equation for the Fermi energy given by [13]

$$E_F^2 = p_F^2 c^2 + m^2 c^4 (1 + 2\nu b) \tag{10}$$

which gives us

$$\nu \leq \frac{E_F^2 - m^2 c^4}{2b m^2 c^4} \tag{11}$$

or

$$\nu \leq \frac{\epsilon_F^2 - 1}{2b} \tag{12}$$

and therefore

$$\nu_m = \frac{\epsilon_{Fmax}^2 - 1}{2b} \tag{13}$$

where $\epsilon_F = \frac{E_F}{mc^2}$ is the unitless Fermi energy and $\epsilon_{Fmax} = \frac{E_{Fmax}}{mc^2}$ is the unitless maximum Fermi energy of the system. Here, the values of ν and ν_m are those values of Landau levels that are fully or partially occupied once all the lower energy levels are completely filled by the electrons with ν_m , in particular, corresponding to the highest Fermi energy chosen *i.e.* E_{Fmax} .

When the electrons fill up all the lower energy states up to the Fermi level, we get the electron number density as [13]

$$n_e = \frac{2b}{(2\pi)^2 \lambda^3} \sum_{\nu=0}^{\nu_m} D_\nu x_F(\nu) \tag{14}$$

where $x_F(\nu) = \frac{p_F(\nu)}{mc}$ is the unitless Fermi momentum defined by

$$x_F(\nu) = [\epsilon_F - (1 + 2\nu b)]^{\frac{1}{2}}. \tag{15}$$

The matter density ρ is related to the electron number density via

$$\rho = \mu_e n_e m_H \tag{16}$$

where μ_e is the mean molecular weight per electron and m_H is the mass of a hydrogen atom. The electron energy density at $T = 0$ K is given by [13]

$$\begin{aligned} \epsilon_e &= \frac{2b}{(2\pi)^2 \lambda^3} \sum_{\nu=0}^{\nu_m} D_\nu \int_0^{x_F(\nu)} E_{\nu, p_z} d\left(\frac{p_z}{mc}\right) \\ &= \frac{2b}{(2\pi)^2 \lambda^3} mc^2 \sum_{\nu=0}^{\nu_m} D_\nu (1 + 2\nu b) \psi\left(\frac{x_F(\nu)}{\sqrt{1 + 2\nu b}}\right) \end{aligned} \tag{17}$$

where

$$\psi(w) = \int_0^w (1 + w'^2)^{\frac{1}{2}} dw' = \frac{1}{2} w \sqrt{1 + w^2} + \frac{1}{2} \ln(w + \sqrt{1 + w^2}). \tag{18}$$

Then the pressure of electron gas in a magnetic field is given by [13]

$$\begin{aligned} P_e &= -\left(\frac{\partial E}{\partial V}\right)_T = n_e^2 \frac{d}{dn_e} \left(\frac{\epsilon_e}{n_e}\right) = -\epsilon_e + n_e E_F \\ &= \frac{2b}{(2\pi)^2 \lambda^3} mc^2 \sum_{\nu=0}^{\nu_m} D_\nu (1 + 2\nu b) \eta\left(\frac{x_F(\nu)}{\sqrt{1 + 2\nu b}}\right) \end{aligned} \tag{19}$$

where

$$\eta(w) = \frac{1}{2} w \sqrt{1 + w^2} - \frac{1}{2} \ln(w + \sqrt{1 + w^2}). \tag{20}$$

The purpose of this paper is to highlight the effects of a strong magnetic field on the DOS of electrons and hence on the EoS of matter inside the star, and eventually to investigate the possibility of strong magnetic fields giving rise to super-massive WD stars that would probably explain the recent observations of the peculiar Type Ia supernovae. Considering this, we restrict our system to at most three Landau levels corresponding to $\nu = 0$, $\nu = 1$ and $\nu = 2$ which will be respectively called a one-level, two-level and three-level system similar to that

done in an earlier work [7]. Each of these systems have a particular value of E_{Fmax} for a chosen magnetic field b or vice versa. The way to do that is to fix ν_m and E_{Fmax} and calculate the value of the B -field from Equation (13). Here, the maximum value of the Landau quantum number ν_m will have values 1, 2, or 3 corresponding to one-level, two-level or a three-level system. For example, this means that for $\nu_m = 3$, all three Landau levels up to $\nu = 2$ are completely occupied by electrons.

Next, we let E_{Fmax} have three values— $2mc^2$, $20mc^2$ and $200mc^2$ and for each of these values we first generate a parametric plot of the EoS—a “ P_e -vs- ρ ” plot corresponding to one-level, two-level and three-level systems of a degenerate electron gas in a magnetic field, since for a given B -field, n_e and P_e are functions of Fermi energy E_F . By doing this, we can also generate a table (Table 1) of values for the variables given in Equation (13). The plot is made by simultaneously solving Equations (14), (16) and (19). Each point on the plot implicitly represents a value of the Fermi energy E_F , and the entire plot is generated by varying E_F from $E_F = mc^2$ to $E_F = E_{Fmax}$ to ensure that the electron gas is relativistic throughout the star, except possibly for a very thin outer crust, which does not affect the main results of our work.

The next step would be to solve the equation of hydrostatic equilibrium of the star under the assumption of spherical symmetry in order to find ρ as a function of radial distance “ r ”. The hydrostatic equilibrium equation is given by [21]

$$\frac{1}{r^2} \frac{d}{dr} \left(\frac{r^2}{\rho} \frac{dP}{dr} \right) = -4\pi G \rho. \tag{21}$$

The pressure due to radiation is neglected here and so is the pressure due to the ionized nuclei which are non-relativistic at the densities found in a typical WD because they are much heavier than electrons. So, $P = P_e$ has been assumed throughout this paper. The above equation can be re-written as

$$\frac{1}{r^2} \frac{d}{dr} \left(\frac{r^2}{\rho} \frac{dP}{d\rho} \frac{d\rho}{dr} \right) = -4\pi G \rho \tag{22}$$

Table 1. Table of variables corresponding to Equation (13).

E_{Fmax}	Maximum Landau levels	b -field
$2mc^2$	1	1.5
	2	0.75
	3	0.5
$20mc^2$	1	199.5
	2	99.75
	3	66.5
$200mc^2$	1	19999.5
	2	9999.75
	3	6666.5

in order to solve for $\rho = \rho(r)$ with a set of two boundary conditions which are given below:

$$\rho_{r=0} = \rho_c \quad (23)$$

$$\left. \frac{d\rho}{dr} \right|_{r=0} = 0. \quad (24)$$

The radius R of the star is given by the first zero of the solution, while the mass M of the star is given by

$$M = \int_0^R 4\pi r^2 \rho dr. \quad (25)$$

3. Correlation between the Plots of the Non-Polytropic Equations of State and Those of the Density of States

Figure 1 shows the plots of the non-polytropic EoS of a cold, degenerate, relativistic electron gas in a magnetic field. Here, an explanation will be given only for $E_{Fmax} = 20mc^2$ because the same explanation applies to the other two values of E_{Fmax} . Consider a one Landau-level system ($\nu = 0$) which corresponds to $b = 199.5$ and is indicated by the solid line. The last point on the curve corresponds to that number density of electrons n_e which completely fills up all the available single-particle energy states of the first Landau level. We can see that the upper part of the curve is much stiffer in comparison to the lower part which is softer. To understand this behavior, we look at Equation (9) for the DOS per unit volume (hereafter referred to as just DOS) in a magnetic field and **Figure 2** which are the plots of the DOS given here in units of $5 \times 10^{31} \text{ cm}^{-3} \text{ erg}^{-1}$. They resemble the DOS of a non-relativistic electron gas in a magnetic field [24]. For the first Landau level corresponding to $\nu = 0$, we essentially have an infinite DOS at $E = 1mc^2$, as can be seen from Equation (9), which then drops off as the energy of the electrons increases when they start to occupy the higher energy states. The area under this curve will give us the number density of electrons.

From the graph of DOS in **Figure 2(a)**, one can see that it becomes more or less steady at a value of about 3.5 (in units of $5 \times 10^{31} \text{ cm}^{-3} \text{ erg}^{-1}$) at about $E = 5mc^2$. For a given B -field, n_e is directly proportional to the Fermi energy E_F . So, when E_F decreases, n_e also decreases. Integrating from $E = 1mc^2$ to $E = 20mc^2$ gives us the total number of electrons per unit volume *i.e.* n_e (~ 70.205 in units of $5 \times 10^{31} \text{ cm}^{-3}$) that will occupy all available states up to $E = 20mc^2$. These electrons have a certain amount of pressure (the degeneracy pressure) as can be seen from the last point on the plot of the EoS (corresponding to $E_{Fmax} = 20mc^2$) for a one-level system-pressure $P_e \sim 2.84 \times 10^{28} \text{ erg} \cdot \text{cm}^{-3}$ and density $\rho \sim 1.17 \times 10^{10} \text{ g} \cdot \text{cm}^{-3}$ or number density $n_e \sim 70.205$. As the Fermi energy decreases, so does n_e and hence the pressure due to all those electrons.

Integrating from $E = 1mc^2$ to $E = 5mc^2$ gives $n_e \sim 17.218$ and integrating from $E = 5mc^2$ to $E = 20mc^2$ gives us $n_e \sim 52.987$. Therefore, we can conclude that for lower energy states up to about $E = 5mc^2$ there are much fewer electrons than those that occupy states from $E = 5mc^2$ to $E = 20mc^2$. Just because

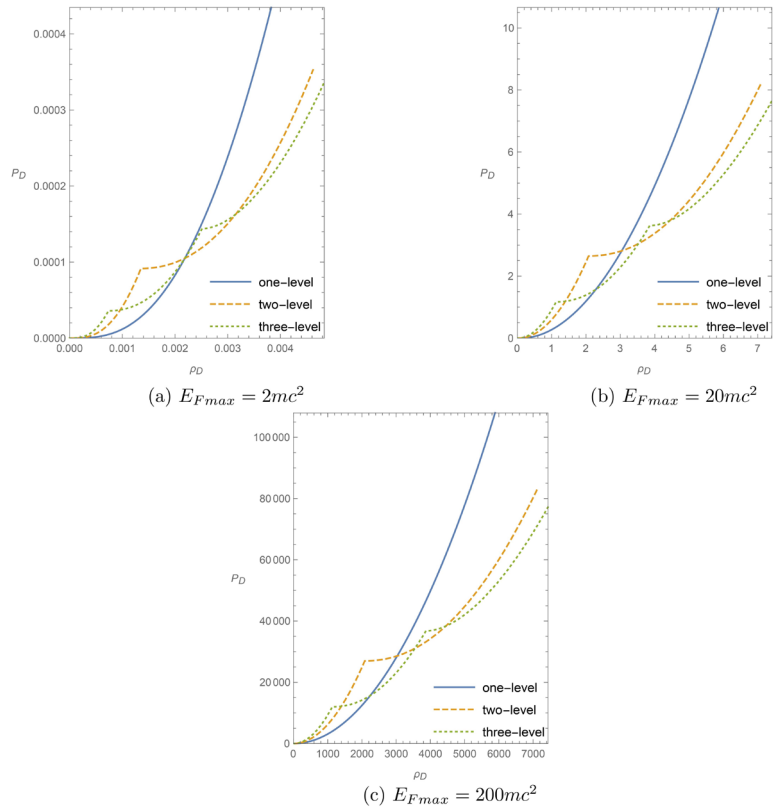


Figure 1. Equations of state in a strong magnetic field plotted for upto three Landau levels for three different maximum Fermi energies E_{Fmax} . Here, P_D and ρ_D are given in units of 2.668×10^{27} erg cm^{-3} and 2×10^9 g cm^{-3} respectively.

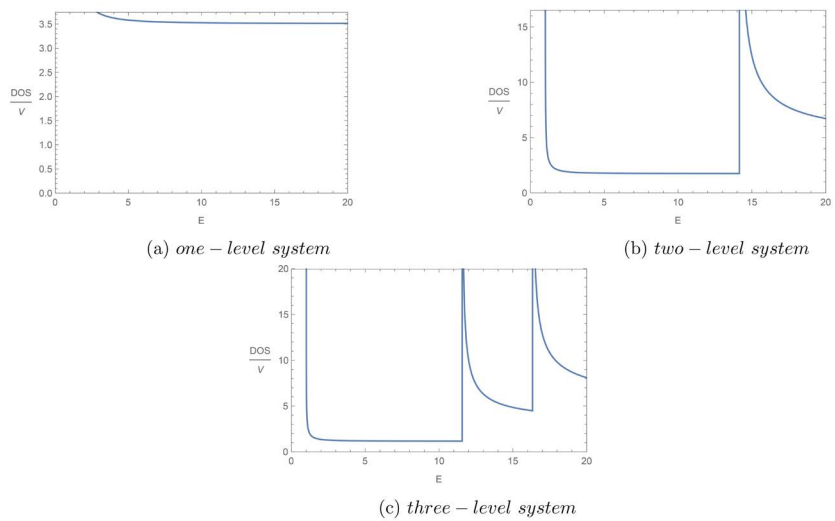


Figure 2. Density of states of a degenerate electron gas in a magnetic field plotted for three Landau levels corresponding to $E_{Fmax} = 20mc^2$. Here, $\frac{\text{DOS}}{V}$ and E are given in units of 5×10^{31} cm^{-3} erg^{-1} and mc^2 respectively.

the DOS is so low (about 3.5) for a significant portion of the energy range, electrons from the energy range $E = 5mc^2$ to $E = 20mc^2$ end up having such higher

energies. Then, combining the contribution of all the electrons, that occupy energy states from $E = 1mc^2$ to $E = E_{Fmax} = 20mc^2$, results in a significant value of pressure (the highest value of pressure in the EoS-plot). The same is also true for electrons occupying states up to lower Fermi energies all the way down from $E_{Fmax} = 20mc^2$ up to about $E_F = 5mc^2$, and hence the resulting graph of the EoS of a one-level system looks “stiffer” for almost the entire density range, except at very low densities from 0 to about $2.9 \times 10^9 \text{ gcm}^{-3}$ (corresponding to $E_F = 1mc^2$ to $E_F = 5mc^2$) in the plot where the curve (EoS) is “softer” due to lesser electrons occupying energy states up to smaller and smaller Fermi energies (up to about $E_F = 5mc^2$).

Basically, when the DOS is low, the electrons occupy energy levels that are not close to each other (similar to the case of a particle confined in a one-dimensional box of infinite potential), and that translates into a steeper rise in pressure with density in contrast to electrons occupying very close-by energy levels when the DOS is high, which translates into a softer rise in pressure with density. So, it is a combination of low DOS and high n_e that results in a steeper rise in pressure for Fermi energies $E_F \gtrsim 5mc^2$ which in turn results in a “stiff” EoS, or that of high DOS but low n_e for $E_F < 5mc^2$ that results in a “soft” EoS.

Essentially, the same explanation holds for two-level and three-level systems as well except that both these systems have, respectively, two and three energy values when the denominator of Equation (9) becomes zero, and we have infinite DOS at those energy values. For a two-level system, one infinity occurs at $E = 1mc^2$ and the second one occurs at about $E = 14.1598mc^2$ which we get by substituting $\nu = 1$ and $b = 99.75$ into the denominator of Equation (9) and equating it to zero. The total number density of electrons at $E_{Fmax} = 20mc^2$ is found, after integrating from $E = 1mc^2$ to $E = 20mc^2$, to be about 84.745. Out of this total, the number of electrons occupying states from $E = 1mc^2$ to $E = 2mc^2$, $E = 2mc^2$ to $E = 14.1598mc^2$, $E = 14.1598mc^2$ to $E = 15mc^2$, and $E = 15mc^2$ to $E = 20mc^2$ are respectively about 3.043, 21.777, 18.876, and 41.047. Once again, because of the way the DOS is distributed as function of energy, the rise in pressure with density due to the electrons is very high, especially due to the total number of electrons that occupy states from about $E = 2mc^2$ to an energy value just below $E = 14.1598mc^2$ (corresponding number density $n_{e2 \rightarrow 14.1598} \sim 21.777$) and then again from about $E = 15mc^2$ to $E = E_{Fmax} = 20mc^2$ ($n_{e15 \rightarrow 20} \sim 41.047$). The same is true for Fermi energies lower than $E_F = 20mc^2$ until about $E_F = 15mc^2$ because as the electrons start to fill the lower energy states, they reach the states at energies from about $E = 14.1598mc^2$ to about $E = 15mc^2$ where the DOS is very high, therefore, many electrons ($n_{e14.1598 \rightarrow 15} \sim 18.876$) end up occupying the states in this energy range which translates into relatively lower rise in pressure with density. The reason why the rise in pressure with density is not much for Fermi energies that fall in this energy range, even when the DOS is very high, is simply because it is a very small energy range, therefore, the electrons end up occupying very close-by energy values in such a small energy range. This is exactly the reason why one

sees a softer EoS for a two-level system in **Figure 1(b)**, in the region to the right of the kink— $\rho \sim 4.15 \times 10^9 \text{ g} \cdot \text{cm}^{-3}$ (value at the kink) to $\rho \sim 7.31 \times 10^9 \text{ g} \cdot \text{cm}^{-3}$ corresponding to $E_F = 14.1598mc^2$ and $E_F = 15mc^2$, respectively. It is this region of the EoS where the pressure does not rise too much with density which is what is termed as having a “soft” equation of state. In a similar manner, we can see that there is also a softening of the EoS at very low densities corresponding to Fermi energies between $E_F = 1mc^2$ and $E_F = 2mc^2$. Thus, there is a direct correlation between the way in which the DOS is distributed as a function of electron energies and the appearance of the EoS-graph. A similar explanation also holds true for a three-level system of a degenerate electron gas where we can see three regions of softening of the EoS (**Figure 1(b)**).

Once the explanation given above is understood, a seemingly surprising fact also becomes clear now when we look at **Figure 1(b)** of the EoS. From this figure, we see that for the one-level system, the last point on the graph corresponds to a density of about $1.17 \times 10^{10} \text{ gcm}^{-3}$ or an electron number density of about $3.5 \times 10^{33} \text{ cm}^{-3}$ while that for a two-level system corresponds to $\rho \sim 1.42 \times 10^{10} \text{ g} \cdot \text{cm}^{-3}$ or $n_e \sim 4.2 \times 10^{33} \text{ cm}^{-3}$ and for a three-level system $\rho \sim 1.48 \times 10^{10} \text{ g} \cdot \text{cm}^{-3}$ or $n_e \sim 4.4 \times 10^{33} \text{ cm}^{-3}$. So, even though, the density is the smallest for a one Landau level system for the same $E_{F_{max}}$, we have the largest value of pressure corresponding to that density value on the graph— $P_e \sim 2.84 \times 10^{28} \text{ erg} \cdot \text{cm}^{-3}$ as compared to $P_e \sim 2.18 \times 10^{28} \text{ erg} \cdot \text{cm}^{-3}$ and $P_e \sim 2.04 \times 10^{28} \text{ erg} \cdot \text{cm}^{-3}$ for two-level and three-level systems, respectively. The way the DOS for a one-level system is distributed as compared to the other two systems *i.e.*, a much larger range of energy values have a drop in the DOS, we can conclude that a one Landau-level system of electrons, even though less dense (at the same value of $E_{F_{max}}$), will end up having much more pressure because of a steeper rise in pressure with respect to density.

4. The Mass-Radius Relations

In this section, we will give an explanation for the mass-radius (M - R) relations of a MWD star corresponding to $E_{F_{max}} = 20mc^2$ and link it to the discussion given in the previous section—Section 3. A similar explanation will also hold true for the other two cases— $E_{F_{max}} = 2mc^2$ and $200mc^2$. **Figure 3** shows the M - R relations for all three levels corresponding to $E_{F_{max}} = 20mc^2$. On all the graphs, each dot represents a star with a particular value of central density ρ_c which is chosen from the different density values from the EoS-plot. Furthermore, as one goes from right to left (on a given branch) in the plot, we find stars with decreasing values of ρ_c . Here, the reader is reminded of the assumptions of spherical symmetry and a uniform and static magnetic field.

4.1. One Landau Level System

First, we take a look at **Figure 3(a)** which shows the M - R relations for a one Landau level system with $b = 199.5$. The end point on this graph is a star with mass $M \sim 2.49M_\odot$ and radius $R \sim 6.68 \times 10^7 \text{ cm}$. This star has a ρ_c equal to

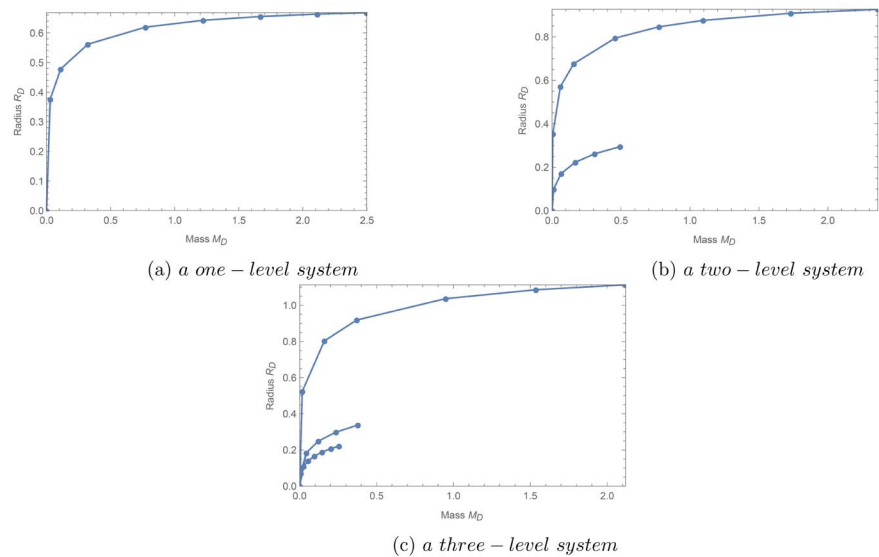


Figure 3. Mass-Radius relations for all three Landau levels corresponding to $E_{F_{\max}} = 20mc^2$. Here, radius R_D and mass M_D are given in units of 10^8 cm and M_{\odot} respectively.

the last density value ($\rho \sim 1.17 \times 10^{10} \text{ g} \cdot \text{cm}^{-3}$) in the EoS-plot for a one-level system. Thus, we see that a high magnetic field can result in a star, the mass of which is significantly higher than the Chandrasekhar limit.

4.2. Two Landau Level System

Next, we look at **Figure 3(b)** which shows the M - R relations for a two Landau level system with $b = 99.75$. Here, we notice something which is not immediately obvious—there are two branches for a two Landau level system. On each branch, again, the stars are shown such that as one goes from right to left, we find stars with a decreasing value of ρ_c . The stars on the lower branch have central densities that are chosen from all those values of densities appearing to the right of the kink in the EoS of a two-level system, with the last (rightmost) star ($M \sim 0.49M_{\odot}$) on this branch having its ρ_c equal to the highest density value in that plot. This branch ends at some non-zero value of mass M and radius R with a particular central density value which is located slightly to the right of the kink, and then we have a jump in the mass-radius values to $M \sim 2.36M_{\odot}$ and $R \sim 9.26 \times 10^7 \text{ cm}$, the rightmost star on the upper branch. This particular star has $\rho_c = 4 \times 10^9 \text{ g} \cdot \text{cm}^{-3}$ which falls to the left of kink, a region of the EoS with only one Landau level occupied.

The subsequent stars on the upper branch have lower masses as well as lower radii, corresponding to further smaller values of ρ_c . This would be a good stopping point for the reader to recall the discussion related to the two-level system given in the previous section. The reason why the highest density value ($\rho \sim 1.42 \times 10^{10} \text{ g} \cdot \text{cm}^{-3}$) of the EoS gives a star with $M \sim 0.49M_{\odot}$ and $R \sim 2.94 \times 10^7 \text{ cm}$ *i.e.*, a star with such a small mass and radius is because of the

softening of the EoS at two places—one just to the right of the kink and the other at densities closer to zero, but more so due to the softening to the right of the kink. Such a star has within it a significant range of densities— $\rho \sim 4.15 \times 10^9 \text{ g} \cdot \text{cm}^{-3}$ to $\rho \sim 7.31 \times 10^9 \text{ g} \cdot \text{cm}^{-3}$ or in terms of dimensionless density, $\rho_D \sim 2.07$ (value at the kink) to $\rho_D \sim 3.65$ in **Figure 1(b)**, where the pressure does not change too much when compared to the much stiffer parts of the EoS. Unitless densities $\rho_D \sim 2.07$ and $\rho_D \sim 3.65$ correspond to $E_F = 14.1598mc^2$ and $E_F = 15mc^2$, respectively. A pressure gradient is required for the hydrostatic equilibrium of a star. Although, we do have a pressure gradient throughout the star, that particular range of densities do not contribute a necessary pressure gradient required by the star to become massive, and hence such a star remains less massive even though it is a star with a ρ_c equal to the highest density value on the EoS-plot. The same explanation also applies to all those stars on the lower branch whose central densities lie on that part of the EoS which is to the right of the kink *i.e.*, when the second Landau level has also started to get filled up. This softening especially affects those stars that have their ρ_c chosen from those density values that lie in the softer region of the EoS *i.e.*, from $\rho_D \sim 2.07$ to $\rho_D \sim 3.65$ (given above), because this range of densities would form the core of these stars, and hence such stars end up being even smaller and less massive.

Moving on to the upper branch, we have a star which is the most massive and has the largest radius even when its central density $\rho_c = 4 \times 10^9 \text{ g} \cdot \text{cm}^{-3}$, which is smaller than the central densities of all the stars on the lower branch. This, again, is possible because of how the DOS looks like up to the energies just below $E = 14.1598mc^2$ (**Figure 2(b)**) because that value of Fermi energy would correspond to a density value just to the left of the kink where the EoS is very stiff. Due to this drop in the DOS, there will be a much steeper rise in the outward pressure due to the electrons (the degeneracy pressure). Also, the somewhat lower pressure gradient region for most stars on the upper branch exists in the outermost layers of the star which are its lowest density regions, and hence would not have a considerable effect on its hydrostatic equilibrium.

4.3. Three Landau Level System

Figure 3(c) shows the M - R relations for a three Landau level system with $b = 66.5$. Following the same trend of explanation as given above for a two-level system, we see that a three-level system results in three branches. Again, the branches are presented in the same manner as for the two-level system with the rightmost star of the bottom-most branch having the highest central density of all the stars in all three branches. This ρ_c would correspond to the last density value ($\rho \sim 1.48 \times 10^{10} \text{ g} \cdot \text{cm}^{-3}$) on the EoS-plot of a three-level system. Not surprisingly, this star has a small mass and radius ($M \sim 0.25M_\odot$ and $R \sim 2.21 \times 10^7 \text{ cm}$). This star has three regions of density where the EoS is softer compared to other regions—one to the right of the highest kink, the second to

the right of the lower kink and the third at very low densities. This star is barely stable due to these three regions inside it, but mainly due to the two softer-EoS regions located to the right of the two kinks in **Figure 1(b)**, and this is why it ends up being less massive and smaller in size as well. This branch ends at some non-zero value of mass M and radius R with a particular central density value located slightly to the right of the highest kink and then we have a jump in the mass-radius values for the middle branch.

For the middle branch, the rightmost star has $M \sim 0.37M_{\odot}$ and $R \sim 3.37 \times 10^7$ cm corresponding to $\rho = 7 \times 10^9 \text{ g} \cdot \text{cm}^{-3}$ which is located to the left of the highest kink. It has a lower mass mainly because of a range of densities within it (located to the right of the lower kink) where the pressure does not change too much as can be seen from **Figure 1(b)** again. The subsequent stars have lower masses as well as radii; exactly the same trend which was seen for the two-level case with the last star having a ρ_c which is equal to a particular value of ρ located to the right of the lower kink (basically from the softer part of the EoS) and having a non-zero but really small mass, and then we have a jump to the topmost branch.

In the topmost branch, the rightmost star has $M \sim 2.11M_{\odot}$ and $R \sim 1.11 \times 10^8$ cm with $\rho_c = 2 \times 10^9 \text{ g} \cdot \text{cm}^{-3}$. This density value is located to the left of the lower kink which is the region of the EoS that is very stiff and where the electrons occupy only the first Landau level.

The other two cases— $E_{F_{max}} = 2mc^2$ and $200mc^2$ will have the same look to their mass-radius plots. They, of course, will have different values of stellar masses and radii for the right-most stars in different branches. **Table 2** summarizes the M - R relations for all three cases. The last column in that table shows the mass-radius values of the rightmost star in a particular branch, and these values are arranged (separated by commas) in rows with the lowest branch first, then the middle one and lastly the upper branch.

Table 2. Mass-radius values of the rightmost star in a branch.

$E_{F_{max}}$	Total branches and Landau levels	Mass-Radius of rightmost star (in units of M_{\odot} and 10^8 cm)
$2mc^2$	1-1	1.32 - 5.54
	2-2	0.37 - 3.08, 0.85 - 6.83
	3-3	0.19 - 2.34, 0.32 - 3.62, 0.81 - 8.01
$20mc^2$	1-1	2.49 - 0.668
	2-2	0.49 - 0.29, 2.36 - 0.93
	3-3	0.25 - 0.22, 0.37 - 0.34, 2.11 - 1.11
$200mc^2$	1-1	2.56 - 0.07
	2-2	0.49 - 0.03, 2.45 - 0.09
	3-3	0.25 - 0.02, 0.45 - 0.03, 2.25 - 0.12

5. Magnetic Momentum-Space and the Shape of the DOS Curve

Because of the significant changes that take place in the \mathbf{p} -space in the presence of a magnetic field, we devote one entire section to explain the magnetic \mathbf{p} -space and the shape of the DOS curve. Those changes in \mathbf{p} -space are responsible for the changes in the DOS, which in turn are responsible for modifying the EoS that leads to a super-Chandrasekhar WD.

Figure 4 shows the \mathbf{p} -space in the absence of a magnetic field. Here, the individual momentum components p_x , p_y and p_z form a continuum. In the absence of B -field, the number of states in a small interval dk in \mathbf{k} -space, where \mathbf{k} is a wave vector, are given by [22]

$$f(k)dk = \frac{d^3k \times 2}{(2\pi/L)^3} = \frac{Vk^2 dk \times 2}{2\pi^2} = \frac{V8\pi p^2 dp}{h^3} = f(p)dp. \tag{26}$$

Here, the spacing of lattice points in \mathbf{k} -space is taken to be $\frac{2\pi}{L}$ by assuming periodic boundary conditions for obtaining solutions to the wave equation in a cubic enclosure of side L and volume $V = L^3$.

In the presence of B -field, we have quantization in the p_x - p_y plane with the radii of the circles given by

$$p_x^2 + p_y^2 = p_\perp^2 = m^2 c^2 \left[2 \left(n + \frac{1}{2} \right) b \right] \tag{27}$$

where p_\perp is the projection of \mathbf{p} onto the p_x - p_y plane. The successive circles correspond to increasing values of the principle quantum number n . For a given n and p_z , the number of free orbitals that coalesce into a single magnetic level *i.e.*, the degeneracy D in the p_x - p_y plane is given by

$$D = \frac{eBA}{2\pi\hbar c} \tag{28}$$

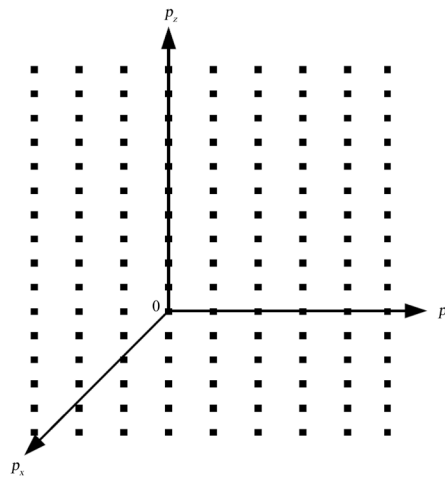


Figure 4. \mathbf{p} -space in absence of a magnetic field. Here, p_x , p_y and p_z values form a continuum.

where A is the area of the orbit (of course, semi-classically speaking) in the x - y plane [23].

Because of the presence of the magnetic field, the quantized three-dimensional p -space gets defined by cylindrical surfaces corresponding to successive values of quantum number n on including the third momentum direction: p_z [24]. The Fermi surface is a sphere that would cut the cylinders, as illustrated in **Figure 5**, to give states that are occupied by electrons with a Fermi momentum belonging to a particular level *i.e.*, $n = 0, 1$ or 2 . For a given B -field, as the Fermi surface grows more and more cylinders are covered by it. One can also see that the Fermi momentum in the z -direction gets smaller as the radius of the cylinder increases *i.e.*, the highest quantum number has the smallest p_F in the z -direction. Also, when the magnetic field becomes very strong, there exists only the ground Landau level corresponding to eigenvalue $n = 0$ *i.e.*, only one cylindrical surface [24].

Now, as an example, when three cylinders corresponding to $n = 0, 1$ and 2 are occupied, the value of DOS at $E = 20mc^2$ in **Figure 6** contains contributions from all those states that lie on the surface of the cylinders, of course, including spin states as well. Because the degeneracy in the p_x - p_y plane is constant, there are a fixed number of states on each circle in **Figure 5**. The number density n_e corresponding to individual Landau levels $\nu = 0, 1$ and 2 in **Figure 6** is respectively $\sim 1.17 \times 10^{33}$, 1.91×10^{33} and $1.35 \times 10^{33} \text{ cm}^{-3}$ or 23.402, 38.215 and 27.022 in units of $5 \times 10^{31} \text{ cm}^{-3}$. For clarity, see also **Figure 7** which shows electron number density n_e plotted as a function of Fermi energy E_F . These values can be explained by recalling Equation (6) and the fact that, except for the Landau quantum number $\nu = 0$, there are two ways in which we can construct a Landau level with quantum number ν . Accordingly, $\nu = 0$ can only be due to $n = 0$ and $\sigma_z = -1$ *i.e.*, all spin-down electron states only, and this shows up as the first value of n_e given above. Basically, these are all the spin-down electrons states that lie on the surface of the innermost cylinder in **Figure 5**. Similarly for $\nu = 1$, we have $n = 0$ and $\sigma_z = 1$ or $n = 1$ and $\sigma_z = -1$ *i.e.*, spin-up electron states from the innermost cylinder and spin-down states from the middle cylinder and they all add up to the second value of n_e given above. Lastly, $\nu = 2$ is due to $n = 1$ and $\sigma_z = 1$ or $n = 2$ and $\sigma_z = -1$ *i.e.*, spin-up states from the middle cylinder and spin-down states from the outermost cylinder combine to given the last value of n_e given above. Naturally, the height of the cylinders in p -space dictates how many momentum states are there on each cylindrical surface *i.e.*, number of states \propto the cylinder height. This is why $\nu = 1$ Landau level has the most electrons. All these facts are clearly reflected in **Figures 5-7** that show individual contributions to the DOS from all three Landau levels.

The discontinuities/infinities in the DOS are due to the fact that as a new level starts to get occupied, new states corresponding to that new Landau level are added at the same energy *i.e.*, the derivative of electron number density with re-

spect to energy $\frac{dn_e}{dE}$ becomes infinite because $dE = 0$, even though $dn_e \neq 0$.

For example, when some value of $p = \sqrt{p_x^2 + p_y^2 + p_z^2}$ corresponding to $n = 0$ becomes equal to that of p_{\perp} of the Landau level $\nu = 1$ with $n = 1$, then the second cylinder in p -space also starts to get occupied at that same energy. The same explanation holds for other levels also.

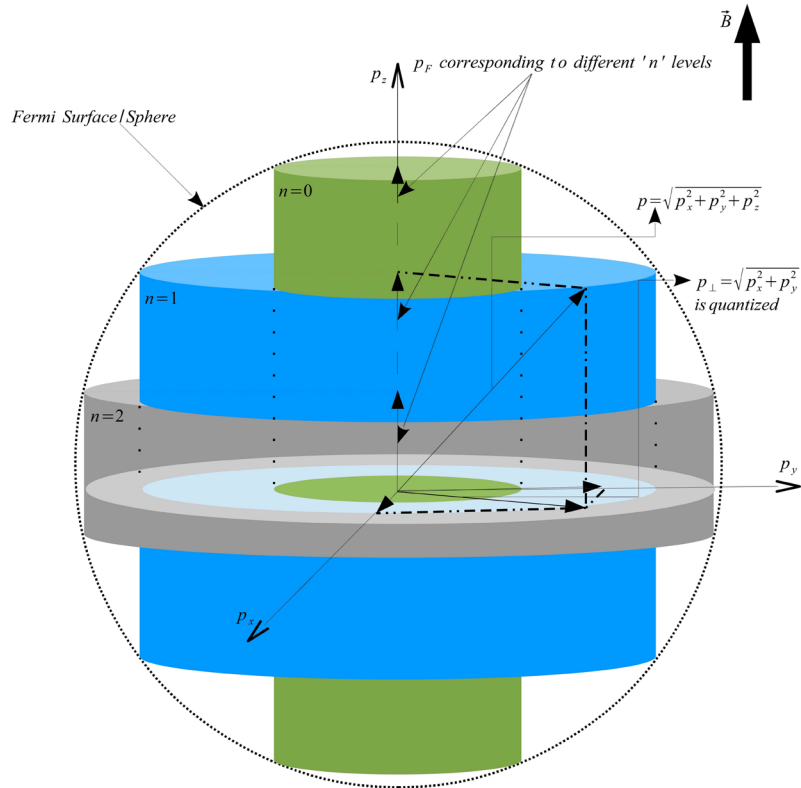


Figure 5. p -space in presence of a magnetic field. Each cylinder is of radius p_{\perp} defined by Equation (27). The radii are not drawn to scale and that implies that the height of the cylinders are also not to scale. Figure is adapted by authors from [24].

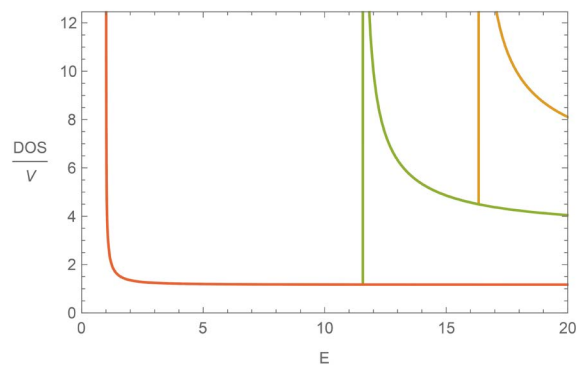


Figure 6. Diagram showing contributions to the density of states per volume from individual Landau levels. A total of three levels are shown here. The $\frac{DOS}{V}$ or $g^*(E)$ and E are given in units of $5 \times 10^{31} \text{ cm}^{-3} \text{ erg}^{-1}$ and mc^2 respectively.

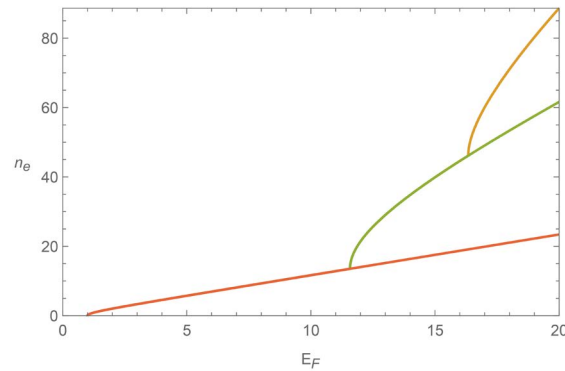


Figure 7. Diagram showing electron number density n_e as a function of Fermi energy E_F for a three-level system corresponding to $E_{Fmax} = 20mc^2$. n_e and E_F are given in units of $5 \times 10^{31} \text{ cm}^{-3}$ and mc^2 respectively.

After every discontinuity in the DOS, we also see that the DOS drops. This can be understood by combining the facts that firstly, the momentum p_z is quantized and secondly, the electron energy eigenvalues are given by Equation (5). Therefore, the higher the value of p_z , the smaller the DOS in a unit energy interval, similar to that in the case of a particle in a 1- d box.

6. Further Explanation for the Super-Chandrasekhar Mass

From Section 4, we saw that a super-massive WD was indeed possible if it had a very strong B -field inside it. What is more interesting is that a super-massive WD was possible when the electrons had occupied only the first Landau level irrespective of the total levels in the EoS—one, two or three. This happens due to the fact that after the infinity in the DOS (in one-level system) and between the first two infinities in the DOS (in two and three-level systems), there is a drop in the DOS to a very small value which allows the electrons that occupy all the energy states up to a certain Fermi energy E_F , which falls within those energy ranges, to exert a higher outward pressure even at significantly lower densities. This was particularly evident in the cases of two and three-level systems.

Also, for the same E_{Fmax} , as the magnetic field goes down the radii of the cylinders corresponding to the quantum number n also goes down (Equation (27)). This means that the degeneracy in the p_x - p_y plane also decreases as can be seen from Equation (28). So, the electrons corresponding to $n = 0$ or $\nu = 0$ level for two and three-level systems start occupying states with non-zero p_z much earlier than those in a one-level system. Hence, such electrons start exerting higher degeneracy pressure (at the same density) sooner compared those in one-level system, and that makes the equations of state of two and three-level systems much stiffer than the one with just one Landau level occupied *i.e.*, only $\nu = 0$. This can be seen from **Figure 1** and **Figure 5**.

These two reasons in the previous two paragraphs, make the EoS related to just the first Landau level very stiff for almost the entire corresponding density range except at very low densities that, anyways, would form the outer layer of

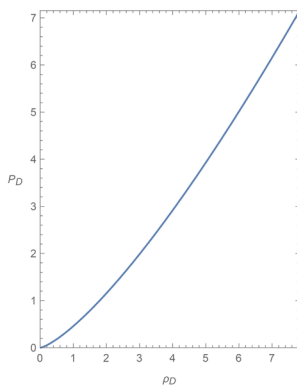
the star and therefore would not matter that much.

For two and three-level systems, the EoS at the highest density also starts out as very stiff, but because of a significant range/s of densities for two/three-level systems within the star where the pressure gradient is not adequate, the star remains less massive even at those higher central densities.

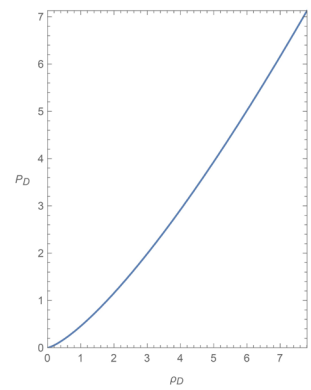
Therefore, it just so happens that a MWD becomes more massive than the Chandrasekhar-limit WD of $1.44 M_{\odot}$ when the electron occupancy is limited to just one Landau level irrespective of the total number of levels in this case of $E_{Fmax} = 20mc^2$.

7. Comparison with the Non-Magnetic Results

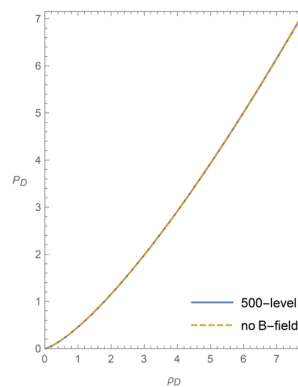
Figure 8 shows the EoS for a 500-level system and a system with no B -field as well as their superimposed equations of state for $E_{Fmax} = 20mc^2$. They look exactly the same proving that, for the same E_{Fmax} , as the magnetic field goes down, the number of Landau levels increases and so the magnetic EoS approaches the non-magnetic one.



(a) $\nu_m = 500$



(b) no B - field



(c) combined

Figure 8. Equations of state for (a) 500-level system, (b) a system with no magnetic field and (c) their superposed equations of state corresponding to $E_{Fmax} = 20mc^2$. Here, P_D and ρ_D are given in units of 2.668×10^{27} erg cm^{-3} and 2×10^9 g cm^{-3} respectively.

Figure 9 shows the M - R relations for a 500-level system. The end point on the curve in this figure corresponds to $M \sim 1.39M_{\odot}$ (which is closer to the Chandrasekhar limit of $1.44 M_{\odot}$) and $R \sim 8.73 \times 10^7 \text{ cm}$. We can also see that for 500-levels there is only one branch. Also, these M - R relations are the same as those of a non-magnetic WD, in the following two aspects [21]:

- 1) Stars are much lighter and do not violate the Chandrasekhar limit.
- 2) The radius of a star decreases as the mass increases.

These can be explained from **Figure 10**. It shows that a magnetic EoS is much stiffer than a non-magnetic one. A stiffer EoS is more successful in counteracting gravity than a softer one (non-magnetic one). That is why MWDs can become more massive than their non-magnetic counterparts. It can also be seen from **Figure 10** that for the same outward degeneracy pressure a non-magnetic electron gas is more dense for almost the entire pressure range. This means that gravitational pressure has a good chance of overcoming the degeneracy pressure, which is exactly what happens in a typical non-magnetic WD. In addition, the non-magnetic EoS being soft, also facilitates gravitational compression. The lower mass stars in **Figure 9** will be bigger because the electron gas, at those densities, would oppose gravity effectively.

Figure 11 shows a comparison of enclosed mass of a star as a function of radial distance r for both a one-level system and a 500-level system. The same central density is chosen for both stars ($\rho_c \sim 1.17 \times 10^{10} \text{ g} \cdot \text{cm}^{-3}$). The mass-radius values for these stars are $M \sim 2.49M_{\odot}$ and $R \sim 6.68 \times 10^7 \text{ cm}$ (one level) and $M \sim 1.38M_{\odot}$ and $R \sim 9.29 \times 10^7 \text{ cm}$ (500 levels). We can see that the star's radius in the case of a 500-level system is bigger even when its mass is much smaller or that of a one-level system is smaller even when its mass is much bigger. This can be explained, again, from **Figure 10**. A stiffer EoS (one-level system) is more successful in counteracting gravity, but that also means that the same degenerate gas has to support more mass. More mass means more gravitational compression. Hence, we have a compact star corresponding to a one-level system. One can clearly see in **Figure 11** that much more mass is enclosed for the same radial distance in the case of a one-level MWD; therefore it has a smaller radius.

From **Figure 12** we can see that the magnetic EoS starts to approach the non-magnetic one when the B -field decreases, even for much fewer Landau levels. The kinks in the EoS get smaller as the number of Landau levels increases for the same E_{Fmax} . We can conclude from all this, that as the number of Landau levels increases (or as the B -field decreases), one no longer finds the same number of branches in the M - R relations as the number of Landau levels in the EoS, but rather the M - R relations evolve in such a way that the number of branches reduces, and ultimately they coalesce to become one branch as can be seen for 500 Landau levels. This is something we can expect since the M - R relations should have just one branch in the limit $B \rightarrow 0$.

We can also expect this because the plot of a magnetic DOS starts to look like

a non-magnetic one when the number of Landau levels increases, as shown in **Figure 13**. One can also notice how the energy ranges in-between the infinities in the DOS become smaller and smaller as the number of Landau levels increases giving the overall appearance of a non-magnetic DOS, as can be seen from **Figure 2** and **Figure 13**. This means that the kinks in the EoS become so small that its overall appearance is of a non-magnetic one. Basically, in **Figure 5**, as the number of cylinders increases for the same E_{Fmax} (or the same sized Fermi surface), the magnetic p -space begins to look like the continuum of a non-magnetic p -space.

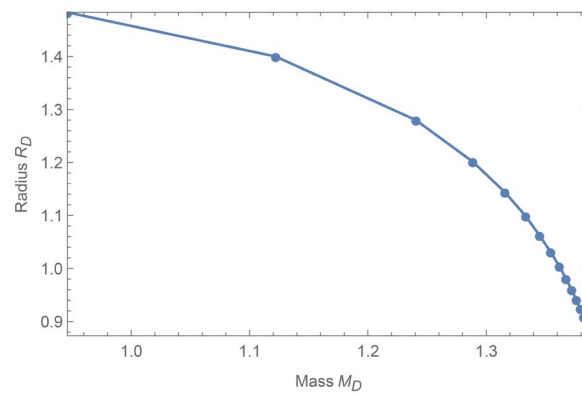


Figure 9. Mass-Radius relations for a 500-Landau level system corresponding to $E_{Fmax} = 20mc^2$. Here, radius R_D and mass M_D are given in units of 10^8 cm and M_i respectively.

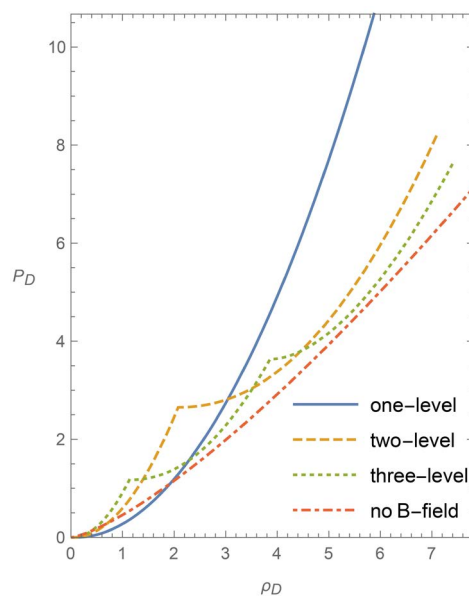


Figure 10. Equations of state for all three Landau level systems as well as for the non-magnetic one plotted for the same maximum Fermi energy $E_{Fmax} = 20mc^2$. Here, P_D and ρ_D are given in units of 2.668×10^{27} erg cm^{-3} and 2×10^9 g cm^{-3} respectively.

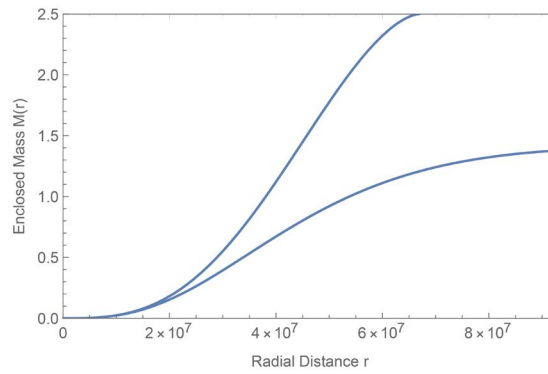
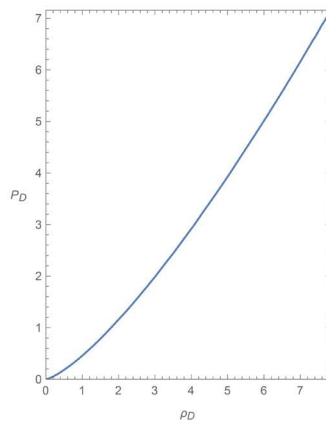
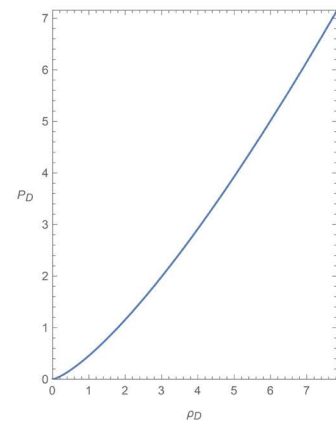


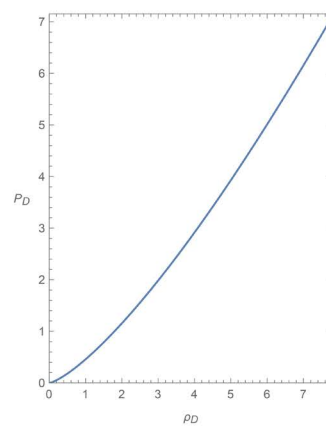
Figure 11. Enclosed Mass v/s Radial Distance of a star for one-level and 500-level systems corresponding to $\rho_c \sim 1.17 \times 10^{10} \text{ g} \cdot \text{cm}^{-3}$. The top curve is of a star with just one-level system. Here, radial distance r and enclosed mass $M(r)$ are given in units of 10^8 cm and M_\odot respectively.



(a) $\nu_m = 50$



(b) $\nu_m = 100$



(c) $\nu_m = 200$

Figure 12. Equations of state for (a) 50-level system, (b) 100-level system, and (c) 200-level system corresponding to $E_{Fmax} = 20mc^2$. Here, P_D and ρ_D are given in units of $2.668 \times 10^{27} \text{ erg cm}^{-3}$ and $2 \times 10^9 \text{ g cm}^{-3}$ respectively.

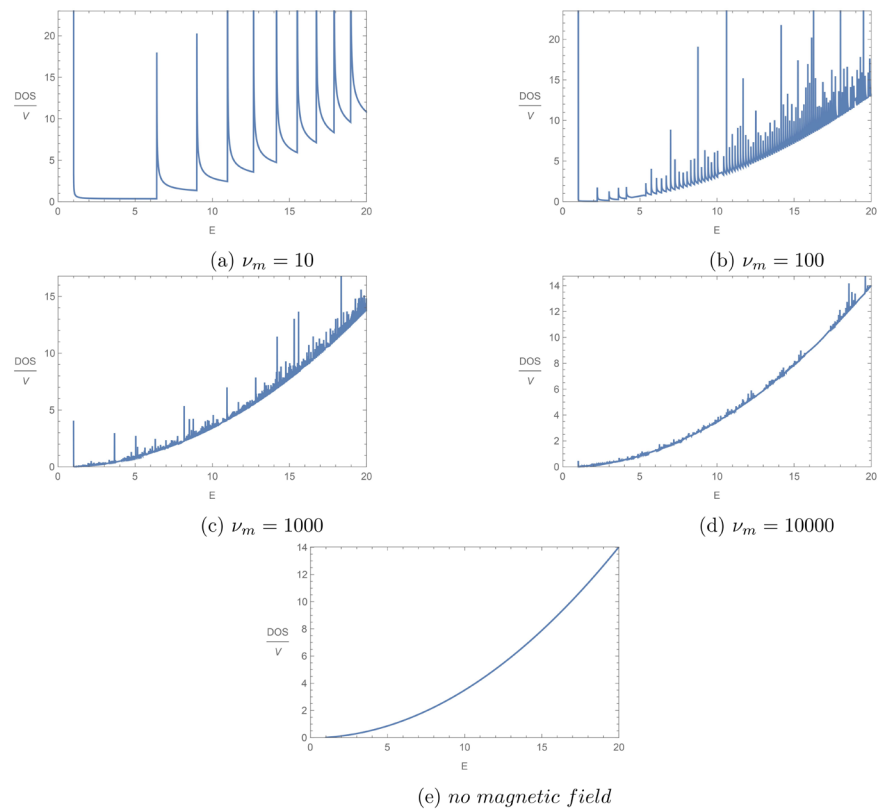


Figure 13. Density of states for (a) 10-level system, (b) 100-level system, (c) 1000-level system, (d) 10,000-level system and (e) system with no magnetic field, all corresponding to $E_{Fmax} = 20mc^2$. Here, $\frac{DOS}{V}$ and E are given in units of $5 \times 10^{31} \text{ cm}^{-3} \text{ erg}^{-1}$ and mc^2 respectively.

8. Comparison with an Earlier Work by Das & Mukhopadhyay (DM)

The main point to discuss in this section is the M - R relations. Because of the correlation between the DOS and the EoS, we have firmly established that a multiple (at least two and three) Landau-level system would lead to multiple branches in the mass-radius relations. This is very different from what DM are proposing [7]. This discrepancy arises due to their incorrect approach in dealing with the EoS. They have done “piece-wise” power-law fits (or polytropic fits as they call them) of the form $P = K\rho^\Gamma$, where $\Gamma = \frac{n+1}{n}$, to the EoS and have wrongly assumed that each individual fit, with particular values of K and Γ , holds throughout the star. Then they have proceeded to numerically solve the equation of hydrostatic equilibrium for ρ as a function of radial distance r , and thus have obtained the mass and radius of the star with one polytropic relation throughout using Equations (21)-(25). This power-law/polytropic relation of the EoS works very well only for a non-magnetic WD where just one such relation would hold [21].

This approach of DM has a serious flaw, in that, they did not make use of the

entire EoS in making stellar models. One can see the presence of unstable masses in their M - R relations. A plausible explanation for that is their incorrect use of the EoS. There are certain regions of the EoS wherein if one assumes a simple power-law/polytropic fit to determine Γ , then one would end up with negative values of densities if that same fit is extrapolated until the pressure becomes zero. Such fits would be from the immediate regions of the EoS that are to the right of the kinks. DM end up with some unstable masses because those negative values of densities end up in the equation of hydrostatic equilibrium (22) for a numerical solution. The equation of state of a MWD is non-polytropic in nature and it would be wrong to assume otherwise.

One can also derive Equations (14) and (19) solely on the basis of quantum mechanics as well as statistical mechanics, and thus does not involve an assumption concerning stars. They together form an “equation of state” for a relativistic degenerate gas no matter where it is found [25]. Once an EoS is generated, that itself describes how the pressure varies with density within a star that has a particular value of a static and uniform B -field within it. So, when a stellar model is generated with a particular value of central density ρ_c , which is chosen from the different density values on the EoS-plot, one has to start with the pressure value corresponding to that chosen value of density at the center of the star. Then the remaining EoS-plot dictates how the pressure varies with density until we reach the surface of the star. We have made proper use of the EoS and have not done “piece-wise” or “polytropic” fits.

9. Conclusions

In this work, we have established a crucial correlation between the DOS and the non-polytropic EoS of a cold, relativistic, degenerate electron gas in a magnetic field which is required to understand the possibility of having super-massive WD stars with strong magnetic fields inside them. We have found how the distribution of single-particle states as a function of electron energies in the presence of a strong magnetic field dramatically changes the EoS of matter inside a MWD star, and renders the star super-massive. In particular, it is only when the electrons occupied the first Landau level that the star became heavier than the Chandrasekhar limiting mass. The drop in the DOS to a very small value in the presence of a B -field for an extended range of energy values is vital in making the pressure gradient very steep, and thus helping to increase the outward degeneracy pressure of the electrons. This was particularly evident in the case of a one Landau-level system.

Although, our results are based on the same assumptions (spherical symmetry, and uniform and static B -field) as made by Das & Mukhopadhyay, they satisfactorily address the observational finding that a magnetic field does lead to an overall higher mean mass of WDs [12]. Such a higher mass of the magnetic WD can only be understood if one looks at the fundamental physics involved, as is done in this work.

We have also found that for two and three-level systems, there are the same number of branches in the M - R relations as there are levels. This, again, was found to be directly related to the DOS. For these levels, the star had density regions inside it where the pressure gradient was not enough to make that star massive even when the central densities were high. The region/s of densities seen to the right of the kink/s in the EoS played a crucial role in this.

One may be puzzled by the discontinuity in the mass-radius values of stars in the branches of the two and three-level systems even as the central densities of stars, starting from the bottom-most branch to the topmost branch, smoothly varied from right to left across the kink/s in their equations of state, however, we have to understand the fact that these stars (stellar models) are built from scratch, guided by the EoS and its dependence on the DOS in the presence of a magnetic field. This is strictly a theoretical model with the assumptions of spherical symmetry and uniform and static B -field. So, it does seem that for multiple Landau levels (at least for two and three levels), there are these jumps in the stellar mass-radius values as the electron occupancy keeps on decreasing to lower levels in a given EoS.

Because we humans cannot reach the stars to perform experiments on them, a critical tool for understanding what might be happening within the stars is via an EoS developed through theoretical models such as that of a cold, relativistic, degenerate electron gas in a magnetic field, as is done in this work.

We believe that we have convincingly tackled this problem of presence of magnetic field inside a star and its consequences from a fundamental perspective. Most importantly, we have succeeded in answering the question—“What is so special about a magnetic field that it makes a white dwarf super-massive?”

Acknowledgements

We would like to thank Dr. Daniel Katz for providing the initial version of the software code for the equation of state and the hydrostatic equilibrium equation.

Conflicts of Interest

The authors declare no conflicts of interest regarding the publication of this paper.

References

- [1] Scalzo, R.A., *et al.* (2010) *The Astrophysical Journal*, **713**, 1073.
- [2] Yamanaka, M., *et al.* (2009) *The Astrophysical Journal*, **707**, L118.
- [3] Taubenberger, S., *et al.* (2011) *Monthly Notices of the Royal Astronomical Society*, **412**, 2735.
- [4] Silverman, J.M., *et al.* (2010) *Monthly Notices of the Royal Astronomical Society*, **410**, 585. <https://doi.org/10.1111/j.1365-2966.2010.17474.x>
- [5] Howell, D.A., *et al.* (2006) *Nature*, **443**, 308.
- [6] Das, U. and Mukhopadhyay, B. (2013) *Physical Review Letters*, **110**, Article ID:

071102. <https://doi.org/10.1103/PhysRevLett.110.071102>
- [7] Das, U. and Mukhopadhyay, B. (2012) *Physical Review D*, **86**, Article ID: 042001. <https://doi.org/10.1103/PhysRevD.86.042001>
- [8] Schmidt, G.D. and Smith, P.S. (1995) *The Astrophysical Journal*, **448**, 305. <https://doi.org/10.1086/175962>
- [9] Schmidt, G.D., et al. (1999) *The Astrophysical Journal*, **512**, 916. <https://doi.org/10.1086/306819>
- [10] Schmidt, G.D., et al. (2003) *The Astrophysical Journal*, **595**, 1101.
- [11] Vanlandingham, K.M., et al. (2005) *The Astronomical Journal*, **130**, 734. <https://doi.org/10.1086/431580>
- [12] Wickramasinghe, D.T. and Ferrario, L. (2005) *Monthly Notices of the Royal Astronomical Society*, **356**, 1576. <https://doi.org/10.1111/j.1365-2966.2004.08603.x>
- [13] Lai, D. and Shapiro, S.L. (1991) *The Astrophysical Journal*, **383**, 745. <https://doi.org/10.1086/170831>
- [14] Ostriker, J.P. and Hartwick, F.D.A. (1968) *The Astrophysical Journal*, **153**, 797. <https://doi.org/10.1086/149706>
- [15] Ginzburg, V.L. (1964) *Soviet Physics—Doklady*, **9**, 329.
- [16] Woltjer, L. (1964) *The Astrophysical Journal*, **140**, 1309. <https://doi.org/10.1086/148028>
- [17] Ferrario, L. and Wickramasinghe, D.T. (2005) *Monthly Notices of the Royal Astronomical Society*, **356**, 615. <https://doi.org/10.1111/j.1365-2966.2004.08474.x>
- [18] Shapiro, S.L. and Teukolsky, S.A. (1983) *Black Holes, White Dwarfs, and Neutron Stars: The Physics of Compact Objects*. 2nd Edition, John Wiley & Sons, New York. <https://doi.org/10.1002/9783527617661>
- [19] Shah, H. and Sebastian, K. (2017) *The Astrophysical Journal*, **843**, 131. <https://doi.org/10.3847/1538-4357/aa74dd>
- [20] Harrison, P. (2005) *Quantum Wells, Wires and Dots: Theoretical and Computational Physics of Semiconductor Nanostructures*. 2nd Edition, John Wiley & Sons, Chichester. <https://doi.org/10.1002/0470010827>
- [21] Chandrasekhar, S. (1958) *An Introduction to the Study of Stellar Structure*. Dover Publications, New York.
- [22] Mandl, F. (1988) *Statistical Physics*. 2nd Edition, John Wiley & Sons, New York.
- [23] Landau, L.D. and Lifshitz, E.M. (1965) *Quantum Mechanics: Non-Relativistic Theory*. 2nd Edition, Pergamon Press, New York.
- [24] Kubo, R., Miyake, S.J. and Hashitsume, N. (1965) *Solid State Physics*, **17**, 269. [https://doi.org/10.1016/S0081-1947\(08\)60413-0](https://doi.org/10.1016/S0081-1947(08)60413-0)
- [25] Harwit, M. (2006) *Astrophysical Concepts*. 4th Edition, Springer, New York.